AD-A195 672 PREDICTION OF TUBE-TUBESHEET GALVANIC CORROSION USING LONG TERM ELECTROCH..(U) DAVID TAYLOR RESEARCH CENTER BETHESDA MD SHIP MATERIALS ENGIN.. J R SCULLY ET AL. 1/1

UNCLASSIFIED MAR 88 DTRC/SME-86-110 F/G 11/6.1 NL

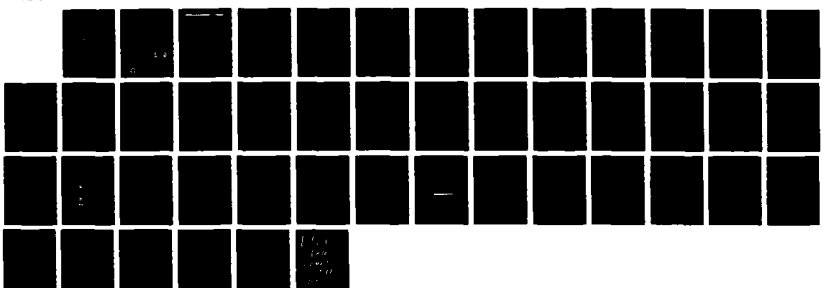

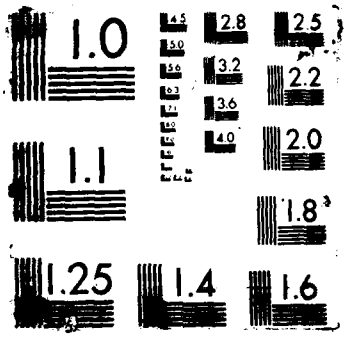
1.0
1.1
1.25
1.4
1.6
1.8
2.0
2.2
2.5
2.8
3.2
3.6
4.0
4.5
5.0
5.6
6.3
7.1
8.0
9.0
10.0

David Taylor Research Center
Bethesda, MD 20084-5000

DTRC/SME-86-110 March 1988

Ship Materials Engineering Department
Research and Development Report

PREDICTION OF TUBE-TUBESHEET GALVANIC CORROSION USING LONG TERM ELECTROCHEMICAL POLARIZATION DATA

by
John R. Scully and Harvey P. Hack

DTRC/SME-86-110 PREDICTION OF TUBE-TUBESHEET GALVANIC CORROSION USING LONG TERM ELECTROCHEMICAL POLARIZATION DATA

MAJOR DTRC TECHNICAL COMPONENTS

CODE 011 DIRECTOR OF TECHNOLOGY, PLANS AND ASSESSMENT

12 SHIP SYSTEMS INTEGRATION DEPARTMENT

14 SHIP ELECTROMAGNETIC SIGNATURES DEPARTMENT

15 SHIP HYDROMECHANICS DEPARTMENT

16 AVIATION DEPARTMENT

17 SHIP STRUCTURES AND PROTECTION DEPARTMENT

18 COMPUTATION, MATHEMATICS & LOGISTICS DEPARTMENT

19 SHIP ACOUSTICS DEPARTMENT

27 PROPULSION AND AUXILIARY SYSTEMS DEPARTMENT

28 SHIP MATERIALS ENGINEERING DEPARTMENT

DTRC ISSUES THREE TYPES OF REPORTS:

1. **DTRC reports, a formal series,** contain information of permanent technical value. They carry a consecutive numerical identification regardless of their classification or the originating department.

2. **Departmental reports, a semiformal series,** contain information of a preliminary, temporary, or proprietary nature or of limited interest or significance. They carry a departmental alphanumerical identification.

3. **Technical memoranda, an informal series,** contain technical documentation of limited use and interest. They are primarily working papers intended for internal use. They carry an identifying number which indicates their type and the numerical code of the originating department. Any distribution outside DTRC must be approved by the head of the originating department on a case-by-case basis.

NDW-DTNSRDC 5602/51 (Rev 2-88)

SECURITY CLASSIFICATION OF THIS PAGE

REPORT DOCUMENTATION PAGE

1a. REPORT SECURITY CLASSIFICATION UNCLASSIFIED	1b. RESTRICTIVE MARKINGS
2a. SECURITY CLASSIFICATION AUTHORITY	3. DISTRIBUTION/AVAILABILITY OF REPORT Approved for public release; distribution unlimited.
2b. DECLASSIFICATION/DOWNGRADING SCHEDULE	
4. PERFORMING ORGANIZATION REPORT NUMBER(S) DTRC/SME-86-110	5. MONITORING ORGANIZATION REPORT NUMBER(S)
6a. NAME OF PERFORMING ORGANIZATION David Taylor Research Center 6b. OFFICE SYMBOL (If applicable) Code 2813	7a. NAME OF MONITORING ORGANIZATION
6c. ADDRESS (City, State, and ZIP Code) Annapolis, MD 21402	7b. ADDRESS (City, State, and ZIP Code)
8a. NAME OF FUNDING/SPONSORING ORGANIZATION NAVSEA 05R25 8b. OFFICE SYMBOL (If applicable)	9. PROCUREMENT INSTRUMENT IDENTIFICATION NUMBER
8c. ADDRESS (City, State, and ZIP Code) Washington, DC 20362	10. SOURCE OF FUNDING NUMBERS PROGRAM ELEMENT NO. 62761N; PROJECT NO.; TASK NO.; WORK UNIT ACCESSION NO. 1-2803-164

11. TITLE (Include Security Classification)
PREDICTION OF TUBE-TUBESHEET GALVANIC CORROSION USING LONG TERM ELECTROCHEMICAL POLARIZATION DATA

12. PERSONAL AUTHOR(S)
John R. Scully and Harvey P. Hack

13a. TYPE OF REPORT	13b. TIME COVERED	14. DATE OF REPORT (Year, Month, Day)	15. PAGE COUNT
Research & Development	FROM _____ TO _____	March 1988	43

16. SUPPLEMENTARY NOTATION

17. COSATI CODES		
FIELD	GROUP	SUB-GROUP

18. SUBJECT TERMS (Continue on reverse if necessary and identify by block number)
Anode, Area ratios, Current density, Cathode, Galvanic corrosion, Flow rate, Galvanic couple, Geometry, (Continued)

19. ABSTRACT (Continue on reverse if necessary and identify by block number)

Quantitative and qualitative predictions of galvanic corrosion rates for tube/tubesheet galvanic couples are presented and discussed. Quantitative galvanic corrosion rate predictions were accomplished using a long-term electrochemical potentiostatic polarization data and finite element analysis. The 120 day potentiostatic polarization data, established for each material in natural seawater, were utilized to incorporate long term polarization/time effects. Corrosion rates were predicted in terms of potential and galvanic current as a function of distance along the length of the tube from the tubesheet. Qualitative galvanic corrosion predictions were made by examining electrochemical polarization data and geometry in the context of the Wagner polarization parameter, under the conditions of secondary and tertiary current distribution.

(Continued)

20. DISTRIBUTION/AVAILABILITY OF ABSTRACT ☐ UNCLASSIFIED/UNLIMITED ☐ SAME AS RPT. ☐ DTIC USERS	21. ABSTRACT SECURITY CLASSIFICATION
22a. NAME OF RESPONSIBLE INDIVIDUAL John R. Scully	22b. TELEPHONE (Include Area Code) 301 267-3151 22c. OFFICE SYMBOL Code 2813

DD FORM 1473, 84 MAR 83 APR edition may be used until exhausted. All other editions are obsolete

SECURITY CLASSIFICATION OF THIS PAGE

★U.S. Government Printing Office: 1988—630-612

Block 18 (Continued)

Conductivity	Concentration polarization	Primary current distribution
Polarization behavior	Mass transport	Secondary current distribution
Tafel polarization	Tube-tubesheet	Tertiary current distribution

Block 19 (Continued)

Seawater exposures of each tube/tubesheet arrangement are compared and contrasted with the predicted results. These exposures used segmented tubes connected in series with zero resistance ammeters. Material combinations exposed included a Monel alloy 400 tubesheet coupled to a 90-10 copper-nickel tube, a 90-10 copper-nickel tube coupled to a zinc anode at the position of the tubesheet, and a nickel-aluminum-bronze tubesheet coupled to an alloy 625 tube. Analysis was also conducted on a nickel-aluminum-bronze tubesheet coupled to a titanium 50 tube, and comparisons are made with similar data reported in the literature.

This paper is directed towards demonstrating the need for accurate electrochemical polarization data to get accurate predictions. The feasibility of finite element analysis for accurate qualitative as well as quantitative galvanic corrosion prediction for the tube/tubesheet configuration is discussed.

CONTENTS

FIGURES

FIGURES (Continued)

FIGURES (Continued)

TABLES

ABSTRACT

Quantitative and qualitative predictions of galvanic corrosion rates for tube/tubesheet galvanic couples are presented and discussed. Quantitative galvanic corrosion rate predictions were accomplished using a long-term electrochemical potentiostatic polarization data and finite element analysis. The 120 day potentiostatic polarization data, established for each material in natural seawater, were utilized to incorporate long term polarization/time effects. Corrosion rates were predicted in terms of potential and galvanic current as a function of distance along the length of the tube from the tubesheet. Qualitative galvanic corrosion predictions were made by examining electrochemical polarization data and geometry in the context of the Wagner polarization parameter, under the conditions of secondary and tertiary current distribution.

Seawater exposures of each tube/tubesheet arrrangement are compared and contrasted with the predicted results. These exposures used segmented tubes connected in series with zero resistance ammeters. Material combinations exposed included a Monel alloy 400 tubesheet coupled to a 90-10 copper-nickel tube, a 90-10 copper-nickel tube coupled to a zinc anode at the position of the tubesheet, and a nickel-aluminum-bronze tubesheet coupled to an alloy 625 tube. Analysis was also conducted on a nickel-aluminum-bronze tubesheet coupled to a titanium 50 tube, and comparisons are made with similar data reported in the literature.

This paper is directed towards demonstrating the need for accurate electrochemical polarization data to get accurate predictions. The feasibility of finite element analysis for accurate qualitative as well as quantitative galvanic corrosion prediction for the tube/tubesheet configuration is discussed.

ADMINISTRATIVE INFORMATION

This project was funded under the Surface Ship Materials Technology Block Program sponsored by the Naval Sea Systems Command (SEA 05R25, Mr. C.A. Zanis) and satisfies milestone RD2.2/3. The work was performed under Program Element 62761N, Task Area SF61541-591, Work Unit 1-2803-164-18.

INTRODUCTION

Prediction of the rate of galvanic corrosion by the use of galvanic corrosion rate tables or by techniques based on electrochemical polarization are useful but

do not take into account current distribution effects. Thus, these methods are only directly applicable when there simultaneously exists in the system of interest 1) a 1:1 anode to cathode area ratio, 2) a high conductivity electrolyte, and 3) a simple geometry with exactly known electrochemically active surface areas. These conditions are necessary to insure that the current is uniformly distributed over both the anode and cathode. For most actual components in service these conditions are not satisfied, and simple prediction methods such as those above cannot be applied. In these instances the distribution of galvanic current is not uniform.

A common geometric configuration that exists on ships where dissimilar metals are used and where galvanic current distribution is not expected to be uniform is the tube and tubesheet configuration in a condenser or heat exchanger. Higher galvanic current densities are expected on the tube surface close to the tubesheet, with the current falling to insignificant levels at some distance away from the tubesheet. For predicting tube corrosion where the tube is more active than the tubesheet, or for predicting tubesheet corrosion if the reverse is true, the distance of galvanic interaction is most important since it changes the effective anode to cathode ratio, which has a significant bearing on the overall corrosion rate of the anode.

Raymond galvanic corrosion MARINE ENGINEERING. (IEE)

In this study galvanic corrosion tendencies of tube/tubesheet combinations in seawater were analyzed utilizing long term potentiostatic polarization curves[1,2] as boundary conditions for finite elements analysis using two different programs: WECAN (Westinghouse Electric Computer Analysis), and MARC. Experimental verification was performed using segmented tubes electrically coupled to tubesheets. The study involved several condenser tube/tubesheet arrangements. 90-10 copper-nickel tubing coupled to a Monel alloy 400 tubesheet, alloy 625 tubing coupled to a nickel-aluminum-bronze tubesheet, and a 90-10 copper-nickel tube coupled to anode grade zinc at the tubesheet position were modelled and tested under quiescent and flowing (2.4 m/s) conditions.

In addition, predicted galvanic current distributions were obtained for a titanium (Ti-50) tube coupled to a nickel-aluminum-bronze tubesheet, and a 90-10 copper-nickel tube coupled to a simulated Muntz metal tubesheet represented by a fixed potential of -250 mV (versus Ag/AgCl). Seawater exposures for comparison in these cases were obtained from available literature. All bimetal combinations investigated are summarized in Table 1.

Table 1. Tube/tubesheet finite element predictions.

Tube Material	Tubesheet Material	Polarization Data		Tube Diameter cm
		Velocity	Time, days	
Alloy 625	Ni-Al-bronze	2.4 m/s	120	2.66
90-10 Cu-Ni	Monel alloy 400	2.4 m/s	120	1.34
Alloy 625	Ni-Al-bronze	2.4 m/s	1	2.66
90-10 Cu-Ni	Monel alloy 400	2.4 m/s	1	1.34
Alloy 625	Ni-Al-bronze	Quiescent	120	2.66
90-10 Cu-Ni	Monel alloy 400	Quiescent	120	1.34
90-10 Cu-Ni	Anode grade zinc	Quiescent	30	1.34
Ti-50	Ni-Al-bronze	Quiescent	1	1.34
90-10 Cu-Ni	-250 mV	2.4 m/s	1	2.66

PREVIOUS WORK

The results of previous investigations are discussed briefly below. The findings of these studies are summarized in Table 2.

Table 2. Summary of tube/tubesheet galvanic corrosion exposures.

Investigators	Material Combination: Anode Tubesheet	Material Combination: Cathode Tube	Galvanic Interaction: Distance, diameters	Velocity: m/s	Time
Astley	Ni-Al-bronze	Titanium	60	1	
	-600 mV SCE	70-30 Cu-Ni	50	quiescent	1 hr
			18	flowing	2 hr
			35	flowing	13 d
Gehring,	-250 mV SCE	AL-6X	120-480	2.1	
Kuester,	-250 mV SCE	AL-29-4	120-480		
and Maurer	Muntz	Ti-50A	120-480		
	Muntz	90-10 Cu-Ni	12-24		
	Muntz	Al-brass	12-24		
Gehring	Muntz	Ti-50A	120-240	2.1	
Gehring	Muntz	Al-6X	120-240	2.1	
and Kyle	Al-bronze	Ti-50A			

Gehring, et al.,[3-5] studied a "simulated" Muntz alloy tubesheet by potentiostatic polarization of tubes to -250 mV versus SCE at the tube inlet. Later, actual Muntz alloy and aluminum-bronze alloy tubesheets were coupled to more noble tube materials in flowing seawater at 7 ft/s (2.1 m/s). Noble tube materials included AL-6X austenitic stainless steel, AL-29-4 ferritic stainless steel, titanium 50 A, 90-10 copper-nickel, and aluminum brass. For both simulated and actual tube/tubesheet studies, cathodic polarization of tube materials along the length of the tube to a distance of 120 to 480 tube diameters was observed for the AL-6X, AL-29-4, and Ti-50A tubes. For couples involving both 90-10 copper-nickel and aluminum-brass coupled to a muntz metal tubesheet, cathodic polarization down the length of the tube was observed for a distance of 12 to 24 tube diameters.

D.J. Astley studied a titanium tube coupled to a nickel-aluminum-bronze plate in seawater flowing at 1 m/s.[6] The length of titanium tube that was cathodically polarized was 60 tube diameters. In a separate study, a 70-30 copper-nickel tube was potentiostatically polarized to -600 mV at the tube inlet, simulating cathodic protection. Under quiescent conditions the length of tube receiving cathodic polarization after one hour was 50 tube diameters. Under flowing conditions after two hours, the length of tube receiving cathodic polarization was 18 tube diameters, but increased to 35 diameters after 13 days.

In summary, the galvanic interaction distance from all studies was found to vary from several tube diameters to several hundred depending upon the materials' polarization behavior, the geometry, and the electrolyte.

NUMBERICAL ANALYSIS FOR GALVANIC CORROSION

Use of finite element and boundary element techniques has shown great promise for predicting potential and current distributions for galvanic corrosion, crevice corrosion, and cathodic protection.[7-14] These techniques are computationally intense, and require powerful computing capabilities for all but the most simple geometries. They require as input the geometry of the configuration of interest and the conductivity of the electrolyte through which current flows. Boundary conditions on free or insulated surfaces are that current cannot flow through the surface, creating a "reflection" effect. At metal surfaces, the polarization characteristics of the metal involved, at the approprieate flow and exposure duration, are used as the boundary conditions. Output from these analyses are potential and current density as a function of position along the structure.

The intent of this study is to demonstrate that tube/tubesheet galvanic corrosion behavior as predicted by finite element analysis depends significantly on the accuracy of long term polarization data and open circuit potentials used for each material in the couple, as well as on the geometry and solution conductivity.

EXPERIMENTAL

TUBE/TUBESHEET EXPOSURE APPARATUS AND PROCEDURE

Two tube/tubesheet combinations were tested, both at quiescent and under flowing (2.4 m/s) conditions. The tubesheet was simulated by a ring of material mounted around, but insulated from, the tube end. This ring was coated on all surfaces except that surface which would face the waterbox in a real condenser. The tube was cut into segments, each insulated from the others, which were shortest close to the tubesheet. The tube segments were electrically connected to each other and to the tubesheet ring with zero-resistance ammeters. Holes were drilled through the tube wall periodically to facilitate installation of micro-reference electrodes for potential measurements. Natural seawater, filtered and maintained at 25°C, was placed in contact with the inside of the tube and the uncoated face of the tubesheet. Current and potential profiles were recorded regularly over a 120 day period. At the conclusion of the quiescent exposure of the copper-nickel tube, this tube was connected to a sacrificial zinc anode and the new current and potential profiles monitored over an additional 30 days under quiescent conditions. The experimental setup is illustrated in Figs. 1 and 2. The two material combinations used were: Alloy 625 tube with Ni-Al-bronze tubesheet, and 90-10 Cu-Ni tube with Monel alloy 400 tubesheet. Dimensions of the tubes and tubesheet rings are listed in Table 3, and the dimensions of the tube segments are listed in Table 4.

POLARIZATION PROCEDURES AND REYNOLDS NUMBER COMPARISONS

Data from 120 day polarization experiments on condenser materials in natural seawater, as described elsewhere[1,2] were utilized as boundary conditions in the finite element analysis programs. In that study, individual samples were held at a constant potential for 120 days. Applied currents were monitored for the duration of the exposure. In the case of the 2.4 m/s flowing seawater polarization data, a Reynolds

number of 30500 was obtained, indicative of turbulent conditions. For the 1.34-cm-diameter-tube configuration described above, an approximately identical Reynolds number was obtained. For the case of the 2.66-cm-diameter tube described above, a somewhat different Reynolds number was obtained, however turbulent flow was still maintained. In addition the maximum change in Nusselt number was estimated to be less than 1.75. This indicates that mass transport conditions are quite similar.

Table 3. Dimensions of tube/tubesheet condensers.

	In 625 Tube/Ni-Al-Bronze Tubesheet	90 Cu-Ni Tube/Monel 400 Tubesheet
R	1.328 cm (0.52 in.)	0.6693 cm (0.2635 in.)
T_1	0.0889 cm (0.035 in.)	0.1245 cm (0.049 in.)
T_2	0.5715 cm (0.225 in.)*	0.2374 cm (0.0937 in.)**
L_1	304.8 cm (10 ft)	304.8 cm (10 ft)
L_2	335.28 cm (11 ft)	335.28 cm (11 ft)

* Calculated based on a tube center to tube center distance of 3.9624 cm (1.56 in.) on a triangular pitch

** Calculated based on a tube center to tube center distance of 2.062 cm (0.812 in.) on a triangular pitch

FINITE ELEMENT ANALYSIS

Finite element analysis was conducted by John Fu at Westinghouse using a program called WECAN on both material combinations tested, but for quiescent conditions only. For this analysis an element mesh shown in Fig. 3 was designed using axisymmetrical (cylindrical) elements to reduce the three-dimensional situation to a two-dimensional analysis. WECAN models polarization by a series of straight lines connecting points on a polarization resistance curve derived from the polarization curve for the material involved at the appropriate flow rate. The polarization resistance is the overpotential divided by the current density at that overpotential, and thus looks like a secant line on the polarization curve connecting the current at the freely-corroding potential to the current at the potential of interest.

Table 4. Segmented tube sections for tube/tubesheet galvanic corrosion analysis.

90-10 Copper Nickel Tube Coupled to Monel Alloy 400 Tubesheet		Inconel Alloy 625 Tube Coupled to Nickel-Aluminum Bronze-Tubesheet	
Distance from Tubesheet (cm)	Tube section Length (cm)	Distance from Tubesheet (cm)	Tube Section Length (cm)
0	1.0	0	3.0
1.0	2.0	3.0	3.0
3.0	3.0	6.0	3.0
6.0	5.0	9.0	3.0
11.0	5.0	12.0	4.0
16.0	25.0	16.0	4.8
41.0	50.0	20.8	5.0
91.0	63.8	25.8	5.0
154.8	75.0	30.8	5.0
229.8	75.0	35.8	8.0
		43.8	8.0
		51.8	8.0
		59.8	9.0
		68.8	10.0
		78.8	10.0
		88.8	10.0
		98.8	10.0
		108.8	26.0
		134.8	30.0
		164.8	30.0
		194.8	40.0
		234.8	70.0

Finite element analysis was also conducted by Raymond Munn at the Naval Underwater Systems Center using a program called MARC. This analysis used a slightly different axi-symmetric mesh, but with roughly the same number of elements. For the MARC analysis, polarization behavior is input by fitting an analytical expression to the actual polarization data. The program then uses the potential at the nearest integration point to substitute into the expression to calculate the current density at any given point on the surface. This current density is then used as the boundary condition for the next iteration in the solution of the problem.

RESULTS

ALLOY 625-Ni-Al-BRONZE CONFIGURATION

The WECAN analysis for the 120 day quiescent case is compared to 120 day experimental data in Fig. 4. There is considerable scatter in the current densities measured, probably due to crevice corrosion of the alloy 625 observed at the conclusion of the test. Considering the scatter, agreement is good between predicted and measured current densities. Qualitative agreement of potential data was considered to be good for the following reason. The interaction distance, the distance after which the effect of the tubesheet on potential and current is minimal, is similar between the predicted and measured data. This distance is about 150 cm, which is about 60-tube-diameters. Therefore, it can be concluded that a large area of cathode is present in this case. A large corrosion rate was predicted for the Ni-Al-bronze and this finding was actually observed once the cell was disassembled. There is, however, some difference between the actual potentials observed and those predicted. This is because the polarization data utilized in the analysis does not have the same open circuit potential for the alloy 625 as the tube material, thus shifting the whole predicted curve below the measured data. Figure 5 illustrates the potential versus time behavior for alloy 625 in quiescent seawater. Note the fluctuations possible even for one sample in quiescent seawater. These fluctuations were considered to be an indication of localized corrosion which was later observed.

The MARC analysis for the 120 day quiescent case is shown in Fig. 6. Since the same polarization data was used in this analysis, the same difficulty in the prediction of potential exists. In spite of this, the interaction distance is about 60 diameters, in agreement with the WECAN analysis and measured potential values as well as the measured experimental currents.

Only MARC was used to analyze this material combination under flowing (2.4 m/s) conditions. Analyses were run using polarization data after one day as well as 120 days. The 1 day data is shown in Fig. 7 and the 120 day as Fig. 8. There is marginal qualitative agreement as to the distances of galvanic interaction in both cases. As with the quiescent data, the freely-corroding potential of alloy 625 used in the analysis appears not to match that actually observed. Figure 8 shows that the interaction distance has decreased 20 diameters due to the flow. This distance is similar between the computer prediction and the measured potentials. Although the 1 day prediction in Fig. 7 (interaction distances of 15 diameters) is similar to the 120 day prediction in Fig. 8, (interaction distance of 25 diameters) the measured potentials are somewhat different. In Fig. 9 the measured tube/tubesheet potential profiles can be seen as they develop over time. The galvanic interaction is initially low (1 day) when the potential difference between the Ni-Al-bronze and the alloy 625 is small, as shown in Fig. 10, and accordingly the galvanic current is low. When the open circuit potential of the alloy 625 increases, the interaction distance increases. However, the galvanic corrosion is more severe at 70 days in this case than with the quiescent case since the cathodic mass transport limiting current density on the alloy 625 is greater under flowing conditions than in the quiescent case. In summary, the tube potentials start out low after 1 day, then increase to a maximum value after 40 days. Then they decrease until 70 days, after which they behave erratically. The systematic shifts in tube/tubesheettreflect the time/potential history of the alloys when freely corroding, as shown in Fig. 10. After 1 day the freely corroding potentials of the alloy 625 and the bronze are similar and relatively low, but the alloy 625 potential rises after a few days, creating higher galvanic currents and higher coupled potentials. After day 70 the alloy 625 potential may have behaved erratically, and the Ni-Al-bronze has

corroded sufficiently to cause the remaining copper surface to exhibit greater passivity, as observed.[2] This explains the confusing time behavior of the 2.4 m/s tube/tubesheet couple reasonable well and points to the necessity for careful consideration of time effects.

90-10 Cu-Ni/MONEL ALLOY 400 CONFIGURATION

The WECAN analysis of this material combination under quiescent conditions at 120 days is presented in Fig. 11. The analysis of this material combination is complicated by the similarity in freely-corroding potentials of the two materials. The predicted interaction distance based on current density is about 10 cm or 8 diameters. The measured interaction distance was closer to 130 cm or 100 diameters after 120 days. The explanation for this behavior seems to be associated with the gradual passivation of the Cu-Ni material which is initially anodically polarized near the tube entrance. The development of a film on this material then promotes the throwing of galvanic current a greater distance down the length of tube. This large discrepancy should be considered in light of the fact that all of the current is at least a factor of 3 below the average general corrosion current for freely-corroding 90-10 Cu-Ni, and therefore both the measured and predicted galvanic effects are insignificant. The difference between predicted and observed potentials once again appears large, but all potentials lie within the observed range of freely-corroding potentials fot the copper-nickel. Thus, the differences are insignificant. Since the increases in anode surface area minimizes the extent of galvanic corrosion, WECAN was successful in predicting an insignificant galvanic corrosion problem.

The MARC analysis for quiescent 120 day conditions in Fig. 12 predicts potentials similar to the WECAN analysis, but an interaction distance more in agreement with that actually measured. The reason for the difference between the two analyses is not known, but MARC was successful in predicting the interaction distance.

Figures 13 and 14 present the MARC analyses and measured potentials under flowing conditions for 1 day and 120 days. Potentials were different between predictions and experimental measurements at both times. In addition, predicted glavanic interaction distances were around 20 diameters after both 1 and 120 days, whereas the observed distance after 1 day was negligible and at 120 days was close to 100 diameters. As in the quiescent case, despite these differences, an insignificant amount of galvanic corrosion between these alloys was predicted as might be expected from the small open circuit potential differences and the area ratio favorable to the anode material.

Figure 15 illustrates the measured tube potential profiles as they develop over time. The potentials start out electronegative at 1 day, then increases so that, with exception of the 60 day data, all potentials are electropositive of the initial values. The reason for this can be seen in Fig. 10. The freely corroding potentials for both alloys increase over the first few days of test. The small potential difference at the beginning few days of the test leads to an insignificant galvanic couple as observed and predicted for the 1 day case. This was reflected in the measured tube potials after 1 day, where no interaction distance could be observed. MARC was successful in predicting a lack of significant galvanic effect under these circumstances. Again, exposure time effects are shown to be quite substantial. In this case of an anodic tube, all errors were on the conservative side, indicated by a large anodecathode area ratio.

90-10 Cu-Ni/ZINC CONFIGURATION

Figure 16 illustrates the results of the MARC analysis for 90-10 Cu-Ni tubing coupled to sacrificial zinc anode material. This prediction is compared to the measured values from this study, keeping in mind that the measurements were on copper-nickel which had already been exposed for 120 days, while the analysis was based on polarization data from only a 30 day exposure. This figure also contains measured data from Astley[6] on a 1.1-cm 70-30 Cu-Ni tube cathodically protected at the end to -600 mV. Interaction distances were 50 diameters fot the prediction, 50 for the measurements from this study, and 40 for Astley's work. This agreement is excellent, considering the differences in the various studies.

OTHER MATERIAL COMBINATIONS

Figure 17 illustrates a potential profile predicted for a 1.34-cm-diameter titanium tube coupled to a Ni-Al-bronze tubesheet. The MARC prediction is based on quiescent polarization behavior after 30 days, and the experimental measurements are for D.J. Astley's 1.46-cm-diameter-tube with 1 m/s flow.[6] Predicted potentials are quite different from those measured. This discrepancy is probably due to a large change in the polarization characteristics of titanium when going from quiescent conditions to a flow of 1 m/s. The prediction is for an interaction distance of over 100 diameters whereas the measured distance was 60 diameters, which is reasonable agreement. In both cases a large cathode to anode area ratio is predicted and galvanic corrosion of the bronze is expected to be severe.

Figure 18 shows a predicted potential distribution on a 134-cm diameter 90-10 Cu-Ni tube at 2.1 m/s coupled to a constant potential source of -250 mV, simulating a Muntz metal tubesheet. The polarization data used for the potential predictions was obtained at 2.4 m/s flow at 1 day. The measured current distribution data is

from work by Gehring,[3-5] who did not report potential distribution. The predicted interaction distance and the measured distance are essentially identical at about 15 diameters. In this case galvanic corrosion is limited to the tube entrance despite the presence of the large cathodic tube surface.

DISCUSSION

QUANTITATIVE PREDICTION BY THE USE OF FINITE ELEMENT ANALYSIS

As described in the preceeding section, agreement between predicted and measured potential profiles is generally not very good. This may be due to sensitivity in the computer analysis to small changes in the shape of the polarization curves used for boundary conditions. Also, the discrepancy may be due to the variable nature of the freely-corroding potential of a material in seawater, which can lead to a displacement of the potential profiles but seems to affect the shape of these profiles only slightly.

Table 5 presents a summary of predicted versus measured interaction distances for all tube/tubesheet combinations discussed above. Interaction distances were measured to range from 15 to 100 diameters, and predicted to range from 8 to 100 diameters. With the exception of one WECAN analysis, measured and predicted inter action distances were very close under quiescent conditions. With the exception of one MARC analysis, measured and predicted interaction distances under flowing conditions were also quite similar. Both exceptions occurred in the tube/tubesheet combination of 90-10 Cu-Ni/ Monel alloy 400, where the total amount of galvanic interaction is extremely small due to similarity in the materials' freely-corroding potentials and the passive behavior of these alloys in seawater. Thus, the finite element technique is a good way to predict the interaction distance down tubes, and

thereby the effective area ratio of a tube/tubesheet galvanic couple. This was the case over a range of material combinations, exposure periods, flow velocities, computer programs, and data sources.

There is insufficient information in this study to make any statement about prediction accuracy for quantitative determination of glavanic corrosion rates.

Table 5. Distances of maximum galvanic interaction.

Tube	Tubesheet	Technique	Interaction Distance (Diameters) Quiescent	2.4 m/s	Time (Days)
Alloy 625	Ni-Al-bronze	Measured	60	15	120
				25	1
		WECAN	60		120
		MARC	60	15	120
				15	1
90-10 Cu-Ni	Monel	Measured	100	100	120
		WECAN	8		120
		MARC	100	20	120
				20	1
90-10 Cu-Ni	Zinc	Meas (Scully)	50		30
		Meas (Astley)	40		1 h
		WECAN	50		30
Ti-50	Ni-Al-bronze	Meas (Astley)	60		
		WECAN	100		30
90-10 Cu-Ni	-250 mV	Meas (Gehring)		15 (2.1 m/s)	
		WECAN		15	1

QUALITATIVE PREDICTION BY THE USE OF WAGNER NUMBER ANALYSIS

The Wagner number[15,16] can be used to evaluate the relative degree of uniformity of current distribution between anodes and cathodes such as galvanic current. This parameter describes the ratio of the kinetic resistance (polarization) to the ohmic resistance (ionic conduction) throughout the electrolyte separating the anode and the cathode as follows:

$$W = \frac{\text{Kinetic Resistance}}{\text{Ohmic Resistance}}$$

When the Wagner number gets very large a uniform current distribution over the anode and cathode is promoted. When the Wagner number gets very small a nonuniform current distribution is promoted. The Wagner number can be changed by modifying either the polarization characteristics of the anode and cathode materials involved, or the solution conductivity, or both, thus changing the uniformity of current distribution. The Wagner number analysis is applicable to primary, secondary, or tertiary current distribution. For the primary case, only the solution conductivity and a characteristic length between anode and cathode are considered:

$$W = K/L$$

where K is the solution conductivity, and L is a characteristic length. In this study the Wagner number was utilized under conditions of secondary and tertiary current distribution, meaning that linear Tafel, and concentration type polarization conditions were all considered as below:

$$W = K\,(\delta\eta/\delta i)_{iavg}/L$$

Table 6 illustrates these various conditions. Note that in the secondary current distribution case a large Tafel coefficient B or B' promotes a large Wagner number, and uniformity of current distribution. In the case of concentration polarization, currents near the limiting current density promote large Wagner numbers. Figures 19 and 20 summarize the various cases of large and small Wagner numbers on the galvanic current distribution for both the case of an anode and a cathode as the tube material, respectively. The exact magnitude of the galvanic current is not determined from the type of treatment. The quantitative solution to these types of problems requires the use of numerical methods as discussed above.

Table 6. Wagner polarization parameter determination.

Current Distribution	Overpotential-Current Relationship		Polarization Resistance Term	Wagner Number
Primary	--		--	K/L
Secondary	$\eta = Bi$	(linear)	B	KB/L
Secondary	$\eta = B' \ln(i/io)$	(Tafel)	B'/i	KB'/iL
Tertiary	$\eta = -RT/nF \ (\ln(1-i/i_L)$	(diff.)	$RT/nF \ 1/(i_L-i)$	$KRT/nF(i_L-i)L$

Figure 21 is the cathode polarization curve for alloy 625 in quiescent seawater. The anodic curve for nickel-aluminum-bronze intersects this curve in the diffusion limited region, which would indicate that the Wagner number should be large for the tube surface, approaching infinity. A large Wagner number should indicate current uniformity, which should result in a large interaction distance on the alloy 625. Observed interaction distances are in fact quite large, 60 diameters. Since titanium has similar polarization characteristics to alloy 625, similar behavior should be observed with couples using titanium tubes. As Table 5 illustrates, Astley measured an equivalent 60diameter interaction distance. Under flowing conditions, the diffusion limited portion of the cathodic curve for alloy 625 should be limited to more more electronegative potentials causing the Wagner number, and the resultant interaction distance, to shrink. This was actually observed, as the interaction distance was only 15-25 diameters at 2.4 m/s flow. Thus, the Wagner number gives a good qualitative indication in this case of the amount of tube surface that has significant effect in the galvanic couple.

Figure 22 is the cathodic polarization and Wagner analysis of copper-nickel in quiescent natural seawater. A galvanic couple between a zinc anode at the position of the tubesheet and a Cu-Ni tube would behave similarly to the above example in quiescent water and produce a large Wagner number, since cathodic currents on the tube are near the limiting current density for oxygen reduction. Large interaction distances are predicted by large Wagner numbers, and were observed at 40-50 diameters both in this study and by Astley, as seen in Table 5.

A Cu-Ni tube coupled to a Muntz metal or similar brass tubesheet would result in a low Wagner number since the cathodic current on the Cu-Ni is far below the limiting current density. This is seen in Fig. 22, where the Wagner number is relatively low at potentials of -250 mV or above. Table 5 shows that Gehring reported only a 15 diameter interaction distance under these circumstances. Again, the Wagner number analysis is a good one for this situation.

The couple between a Cu-Ni tube and a Monel alloy 400 tubesheet will result in a low Wagner number, as illustrated schematically in Figs. 22 through 24. This should result in galvanic current being limited to the entrance of the anodic tube. Low interaction distances are predicted in this case, but in this study the observed interaction distances are very large, 100 diameters. This can only be explained if the tube material becomes passivated, in which case the Wagner parameter becomes large for the anode tube material and the current becomes more uniform.

The experimental results not modelled here, but reported in Table 2 can also be analyzed using the Wagner number. Following the same logic used above, a large interaction distance is predicted for all studies in this table except those involving copper-nickel or brass. With only 2 exceptions from Astley's work, the interaction distances were all observed to be from 50-480 diameters, in agreement with the prediction. The copper-nickel and brass couples are all predicted to have short interaction distances, and all were reported in the range of 12-24 diameters.

The above analyses indicate how good a predictor the Wagner number is for estimating in teraction distances in tube/tubesheet galvanic couples. Although quantitative prediction is not possible using this analysis, qualitative information can be gained, which is useful for determining the effects of exposure variables on interaction distance. This can be accomplished by examining the effects of these variables on polarization behavior and determining Wagner numbers as a function of potential.

CONCLUSIONS

Quantitative predictions of galvanic corrosion by finite element methods can be accomplished by predicting distances of galvanic interaction provided that long term electrochemical polarization data and open circuit potential behavior are carefully considered and incorporated into such analysis. Without consideration of potential-current-time effects resulting predictions may be misleading or in error. Qualitative indications of galvanic corrosion interaction distances may be obtained through utilization of the Wagner number analyzed in the case of the primary or secondary current distribution. Consideration of potential-current-time effects are still required and no quantitative data may be yielded through this method.

ACKNOWLEDGEMENTS

The authors would like to thank the staff of the LaQue Center for Corrosion Technology for conducting experimental verifications. They would also like to thank Dr. J. Fu, formerly of Westinghouse R&D Center and Mr. Raymond Munn of Naval Underwater Systems Command for their finite element analysis work.

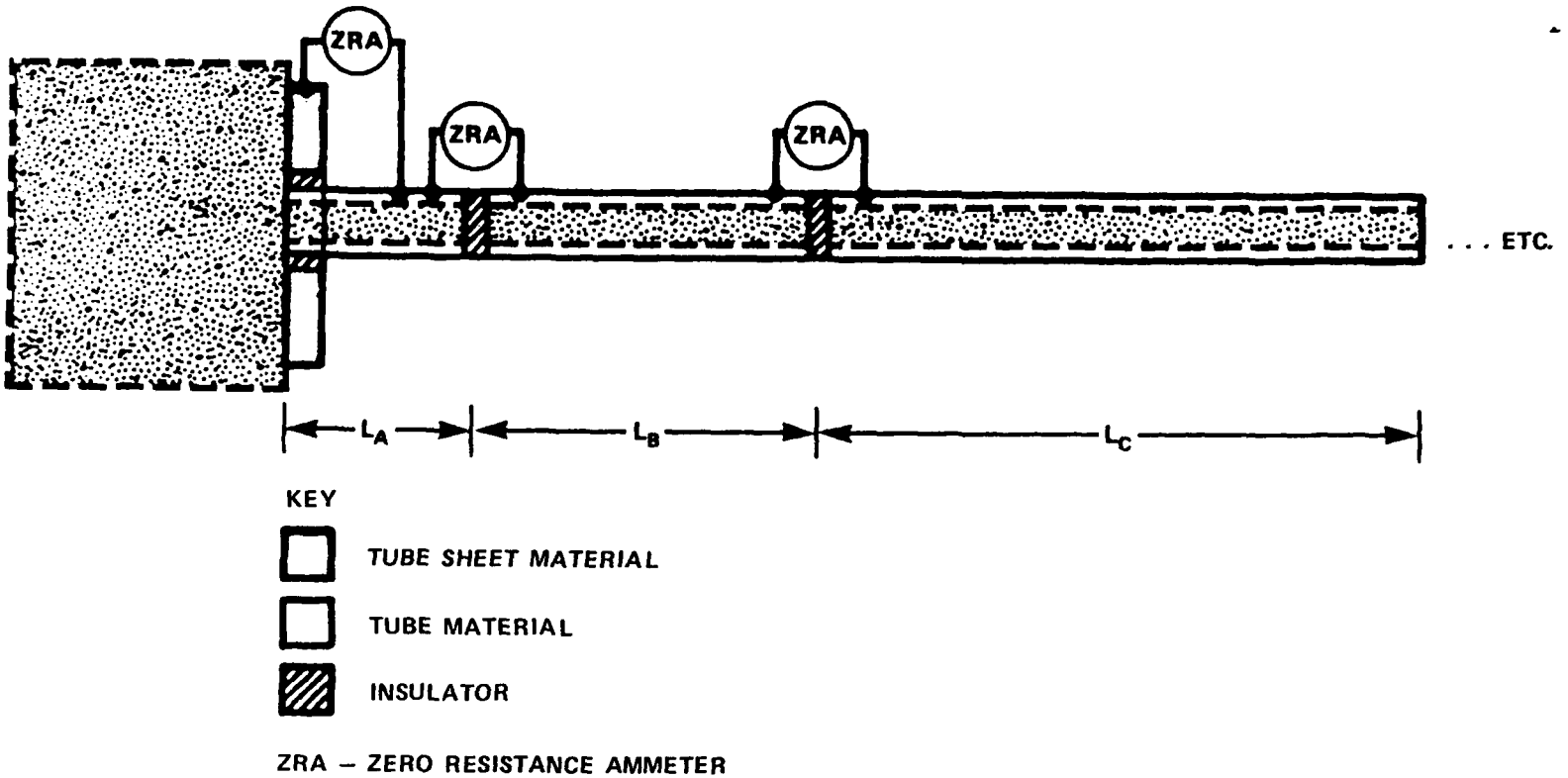

Fig. 1. Schematic of segmented tube galvanic corrosion experiment.

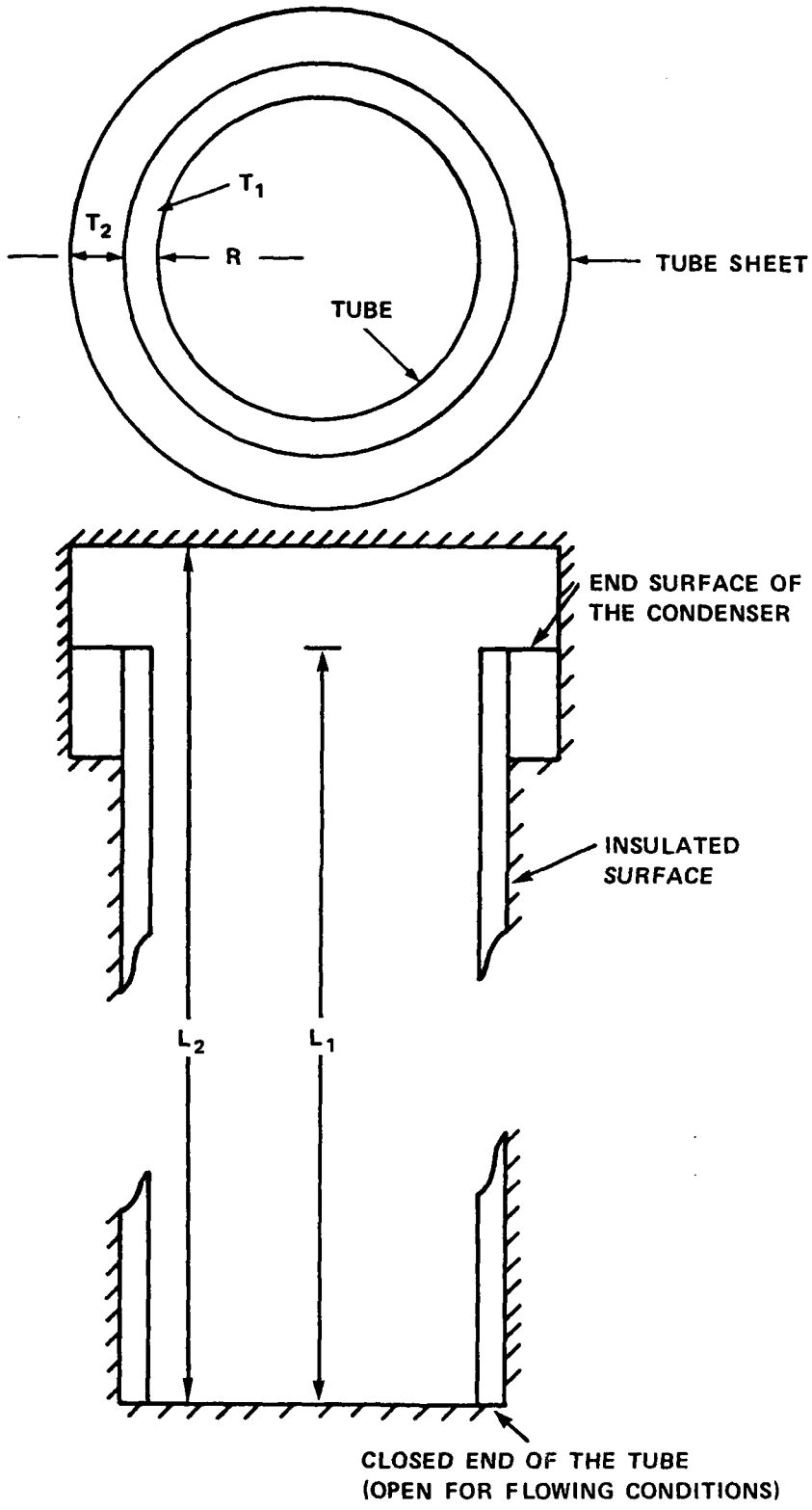

Fig. 2. Schematic seawater cooled condenser.

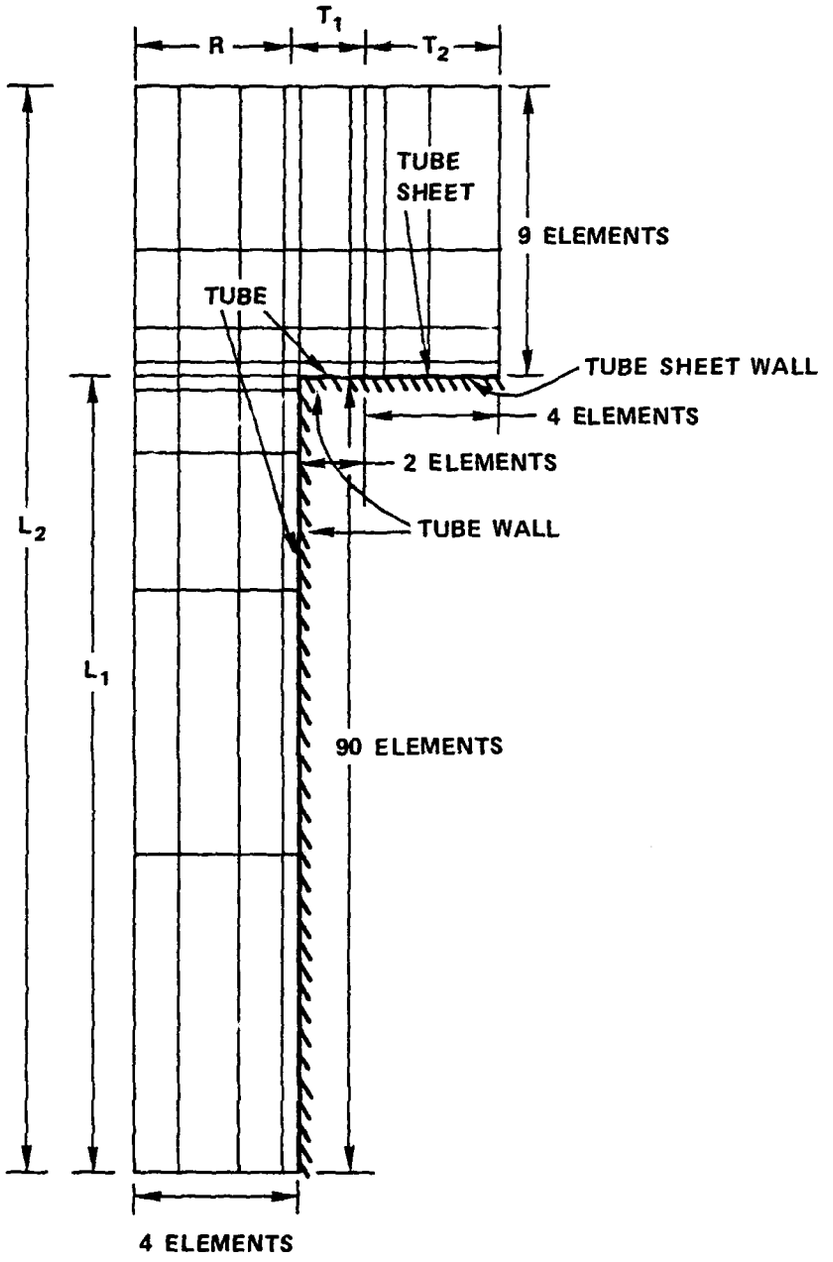

Fig. 3. Finite element mesh with axisymmetric elements used to reduce 3D geometry to 2D.

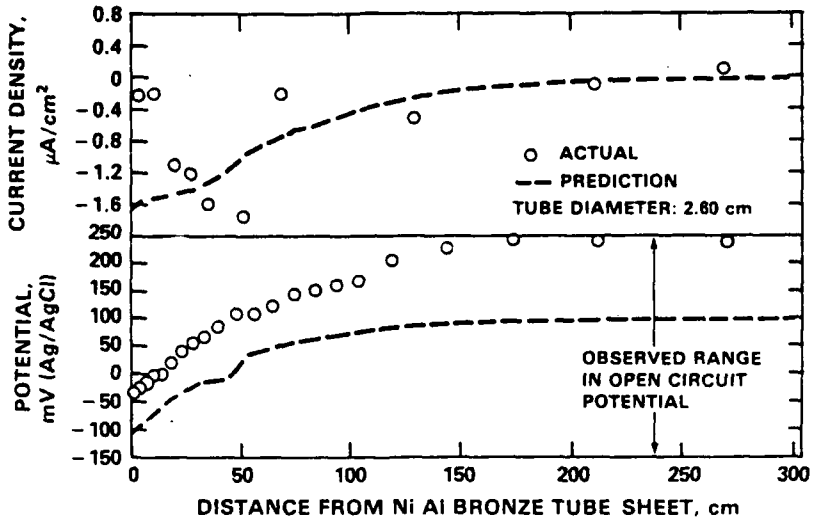

Fig. 4. Current and potential distribution on alloy 625 tube after 120 days.

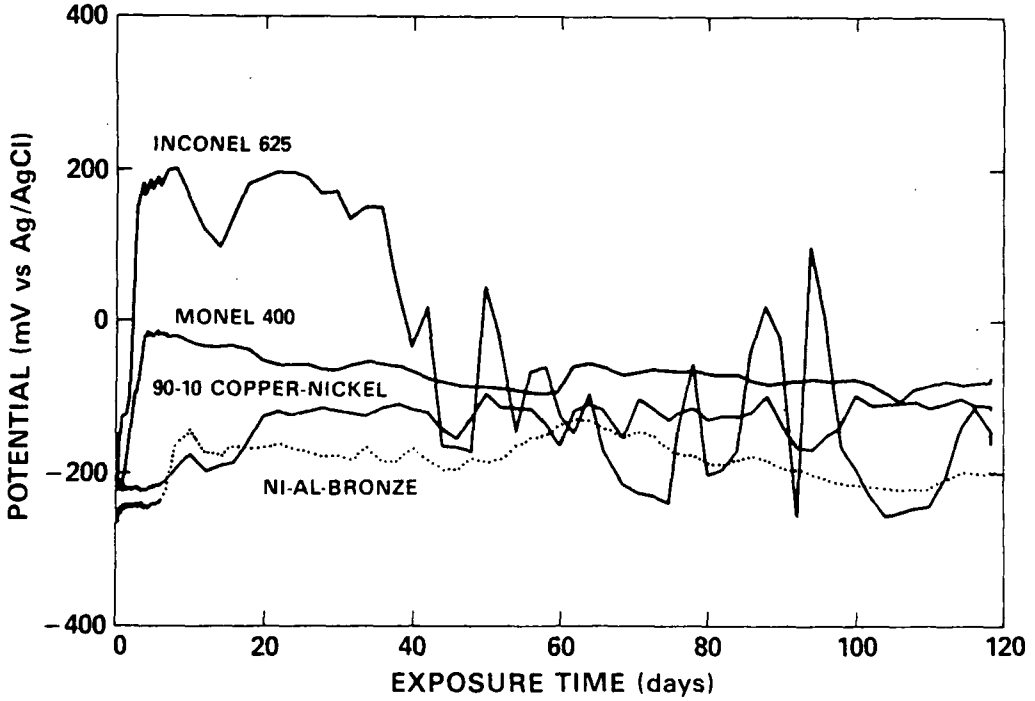

Fig. 5. Potential versus time behavior for alloy 625 and Ni-Al-bronze in quiescent seawater.

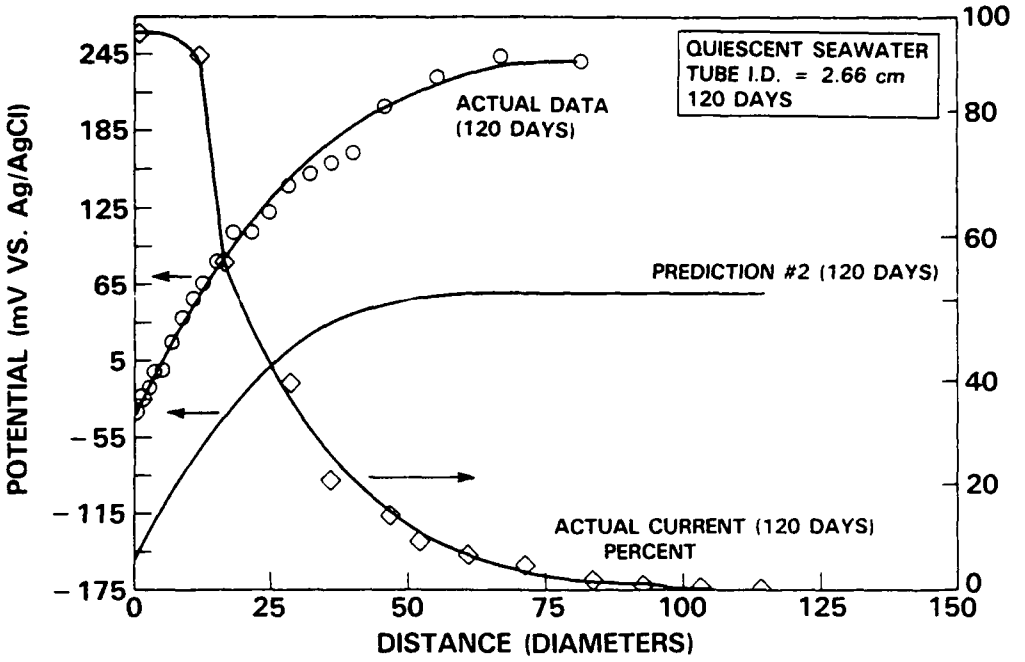

Fig. 6. Galvanic corrosion behavior for an alloy 625 tube coupled to Ni-Al-bronze: quiescent 120 days.

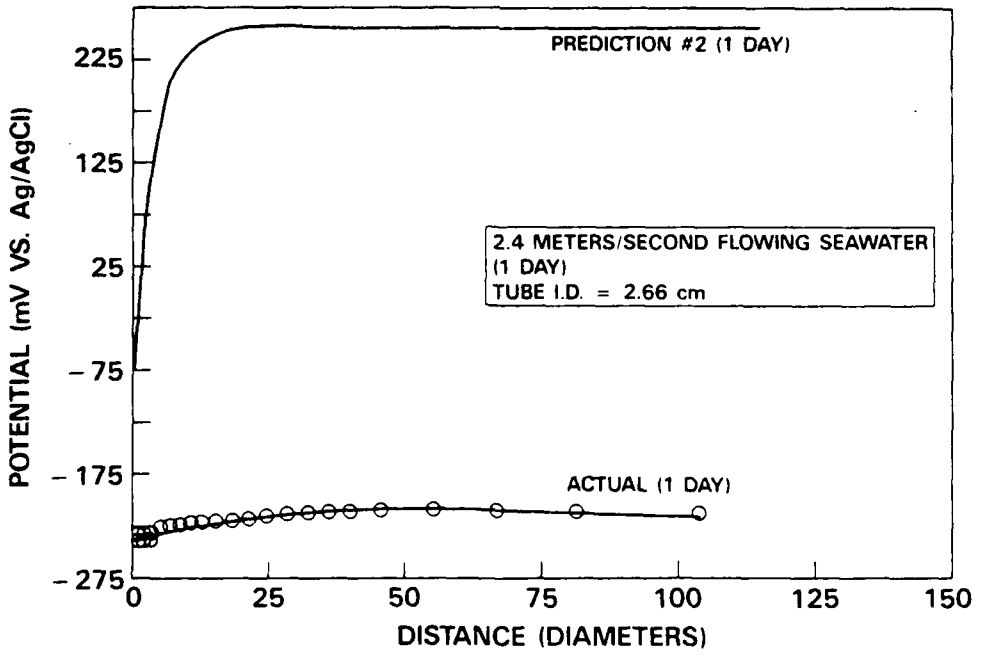

Fig. 7. Galvanic corrosion behavior for alloy 625 tube coupled to Ni-Al-bronze tubesheet: flowing 1 day.

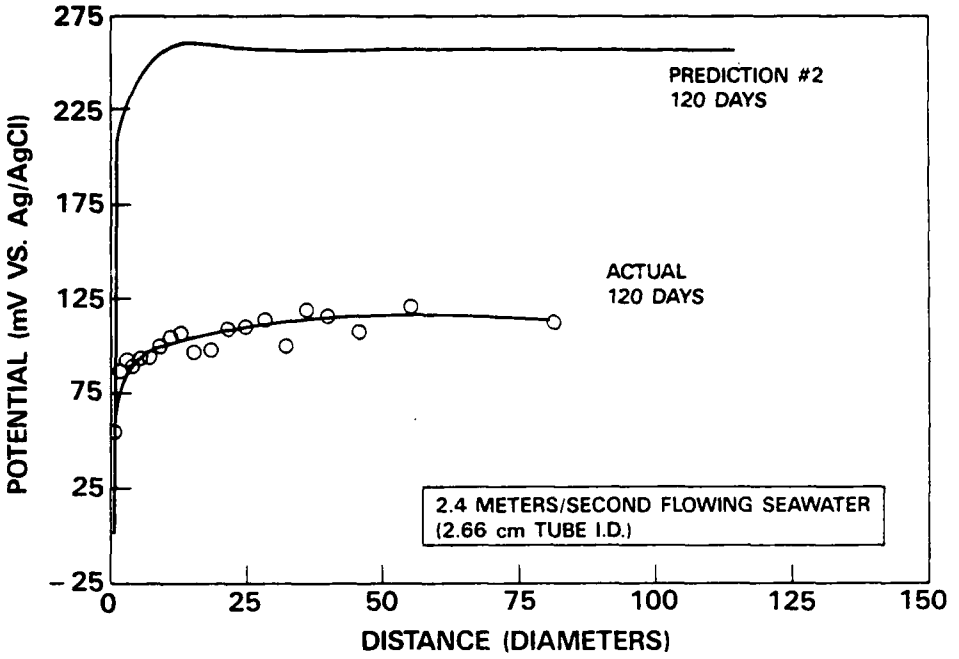

Fig. 8. Galvanic corrosion behavior for alloy 625 tube coupled to Ni-Al-bronze tubesheet: flowing 120 days.

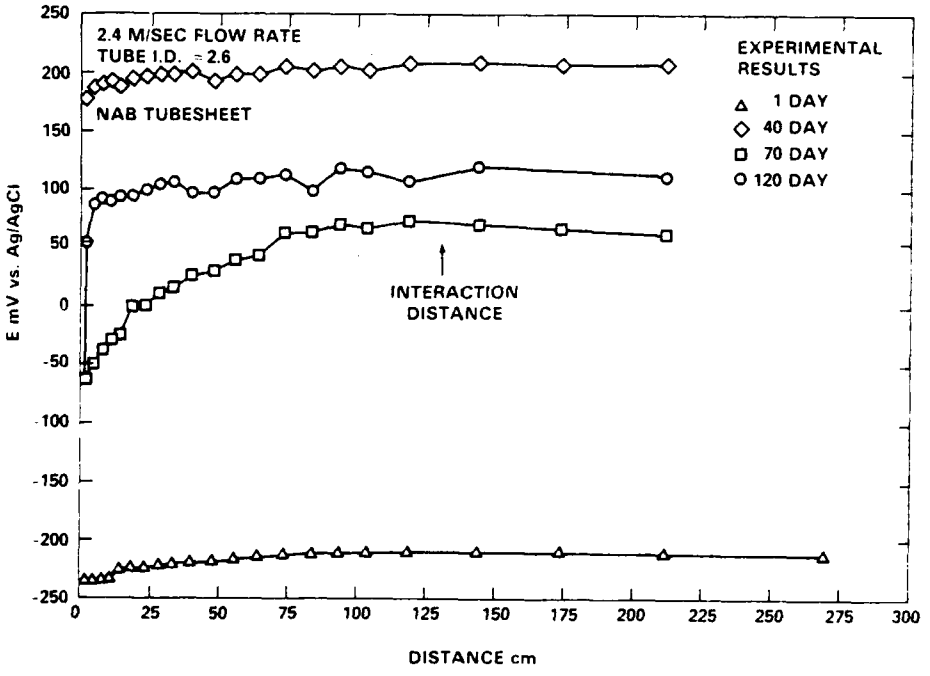

Fig. 9. Galvanic corrosion behavior time effects for alloy 625 tube coupled to Ni-Al-bronze tubesheet: flowing 1 to 120 days.

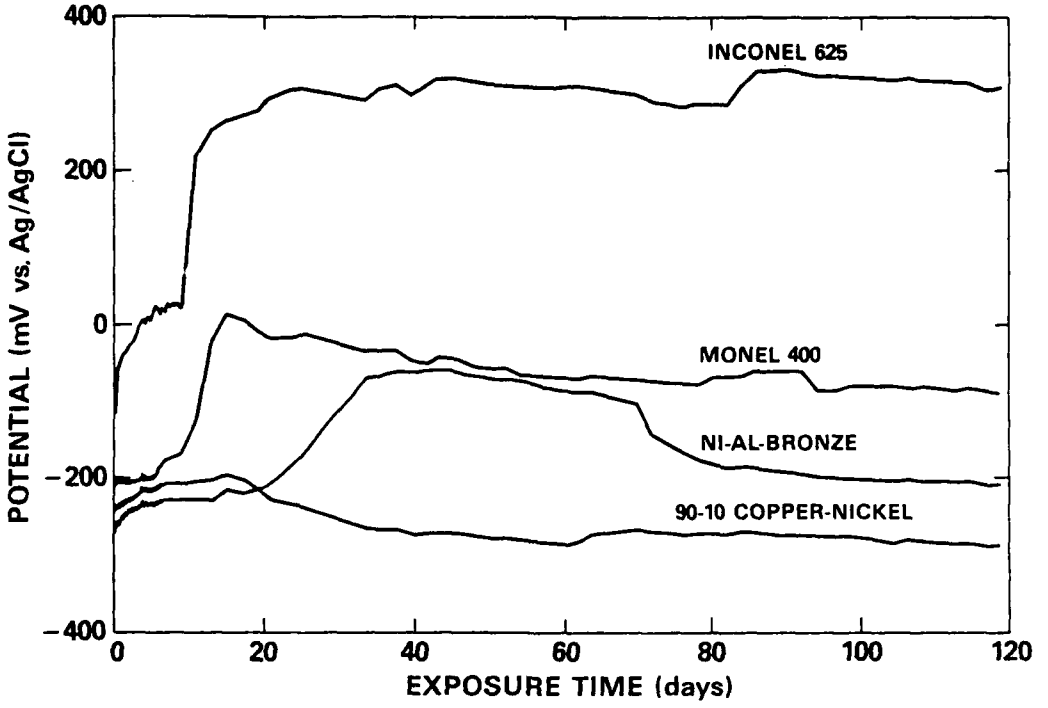

Fig. 10. Potential versus time behavior for tube and tubesheet materials in flowing seawater.

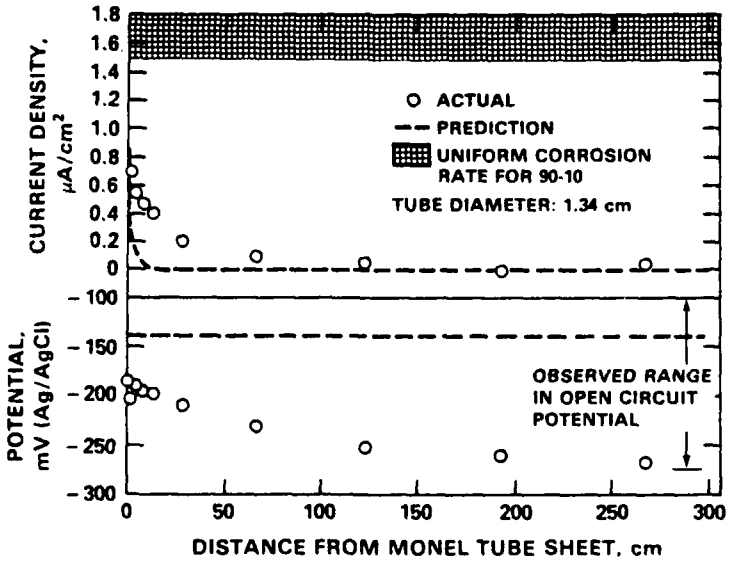

Fig. 11. Current and potential distribution on 90-10 Cu-Ni tube after 120 days in quiescent seawater.

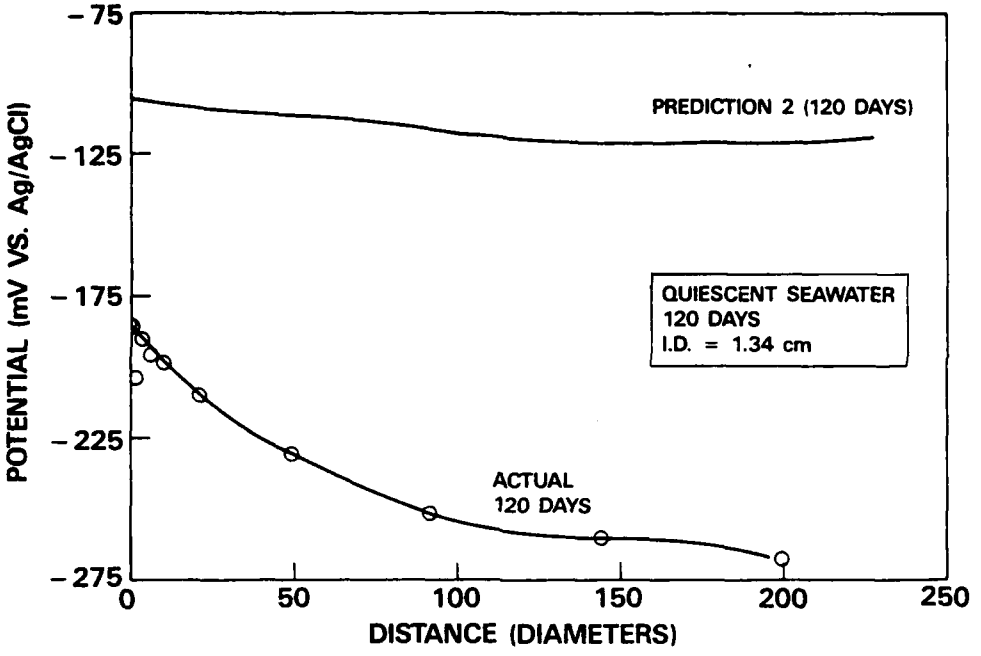

Fig. 12. Galvanic corrosion behavior for a 90-10 Cu-Ni tube coupled to Monel alloy 400: quiescent 120 days.

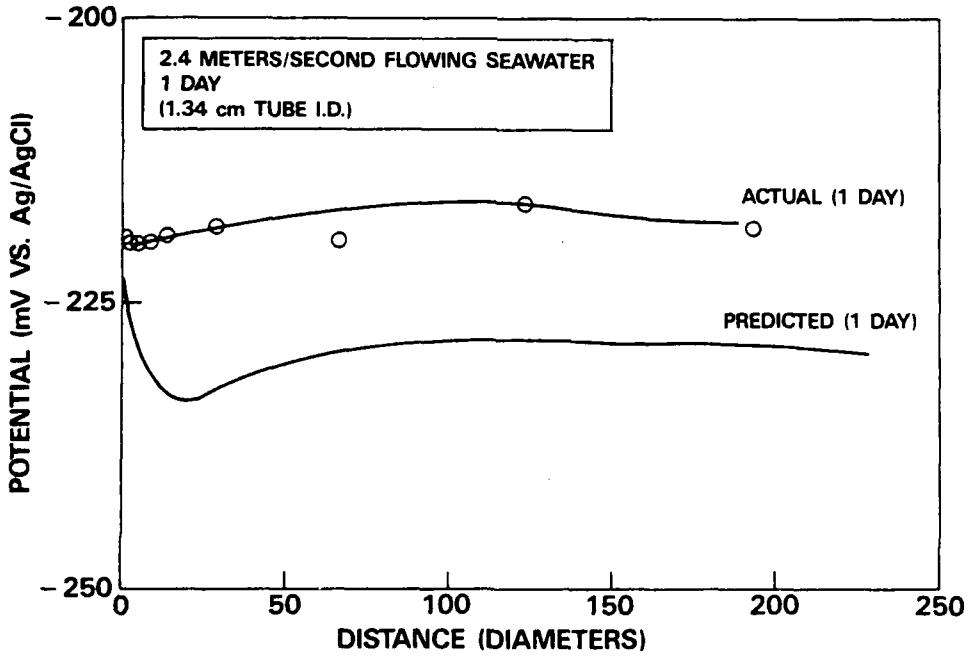

Fig. 13. Galvanic corrosion behavior for a 90-10 Cu-Ni tube coupled to Monel alloy 400: flowing 1 day.

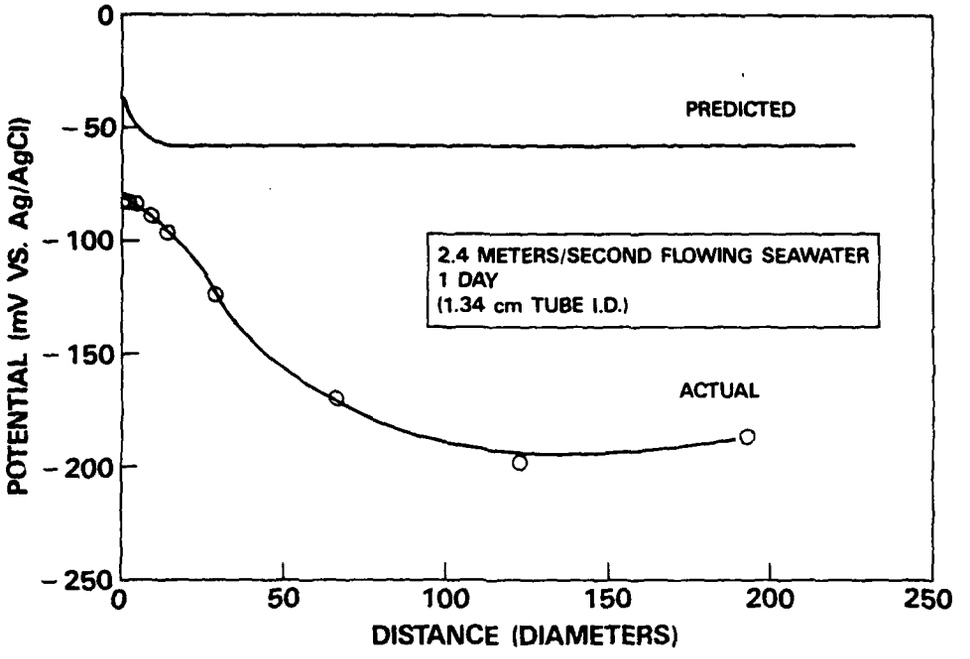

Fig. 14. Galvanic corrosion behavior for a 90-10 Cu-Ni tube coupled to Monel alloy 400: flowing 120 days.

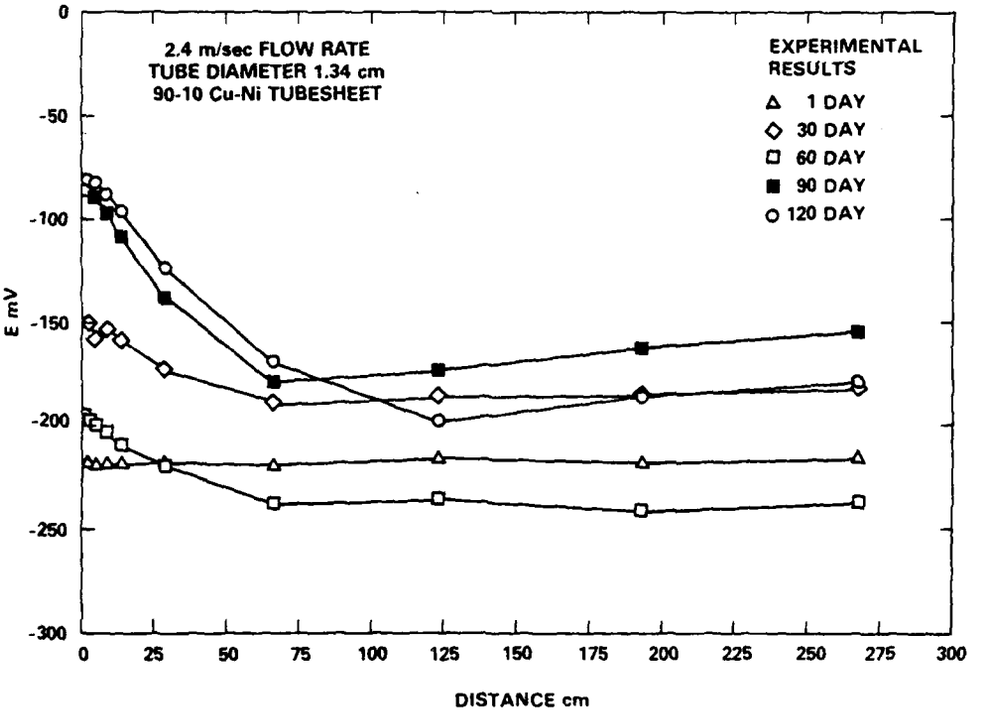

Fig. 15. Galvanic corrosion behavior time effects for 90-10 Cu-Ni tube coupled to Monel alloy 400 tubesheet: flowing 1 to 120 days.

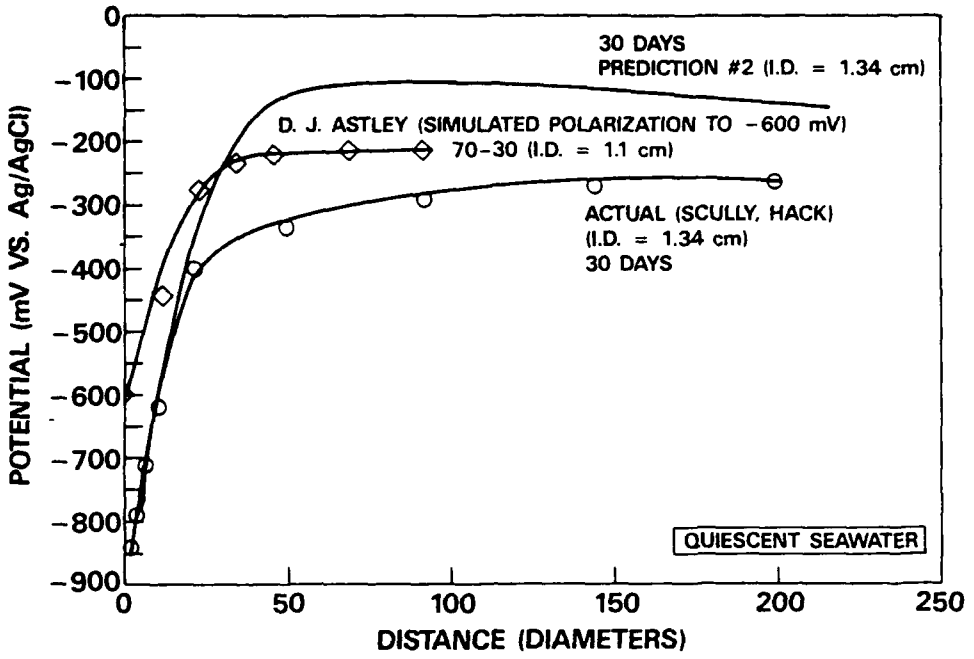

Fig. 16. Galvanic corrosion behavior for 90-10 and 70-30 Cu-Ni tubes coupled to anode grade zinc at the tubesheet.

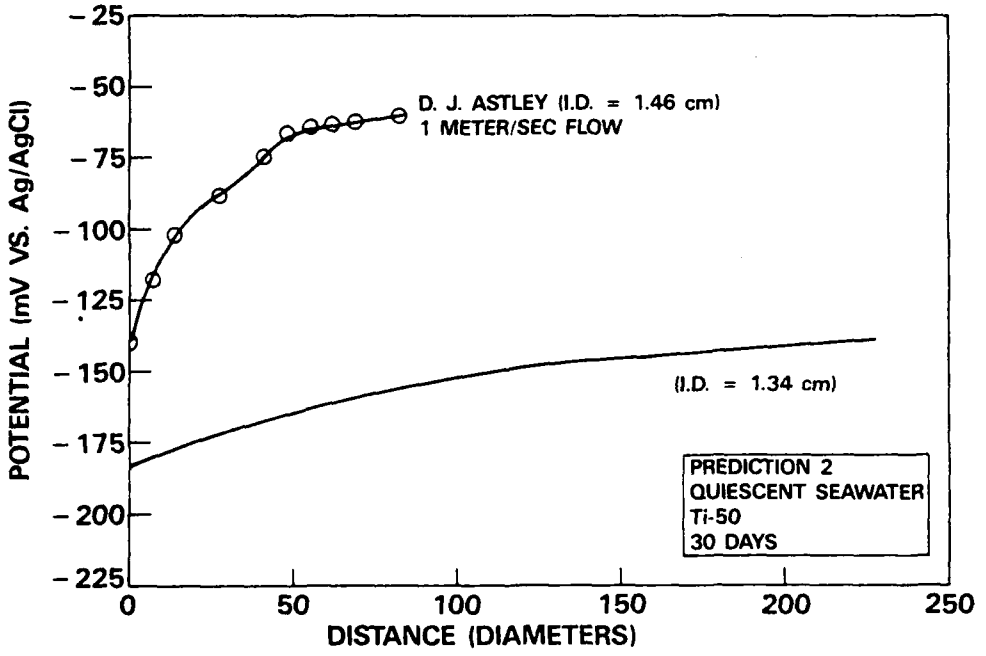

Fig. 17. Galvanic corrosion behavior for a titanium tube coupled to Ni-Al-bronze tubesheet.

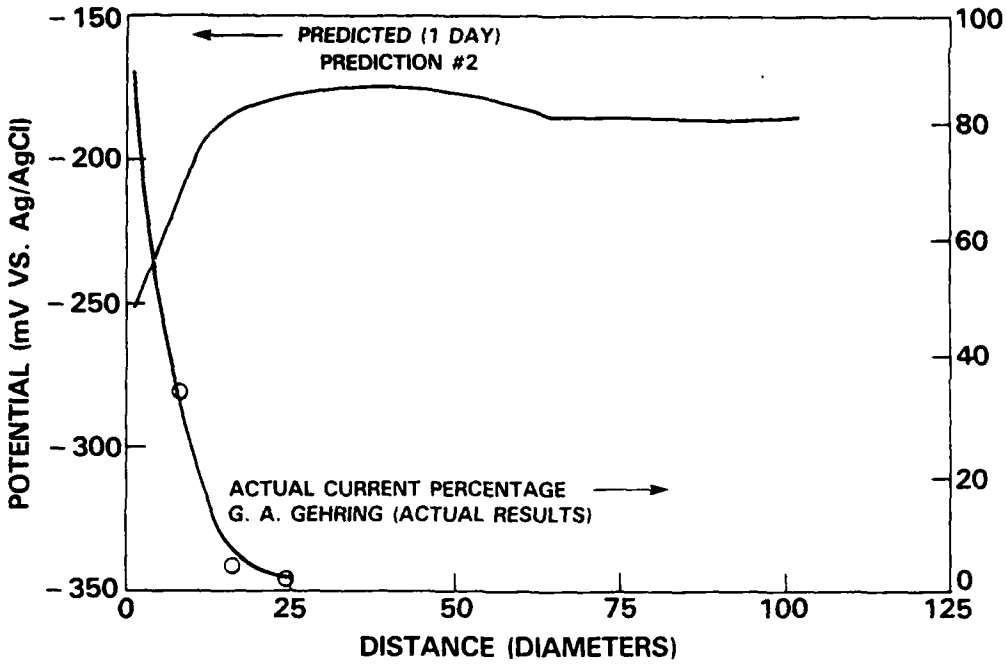

Fig. 18. Galvanic corrosion behavior for a 90-10 Cu-Ni tube coupled to Muntz metal alloy tubesheet.

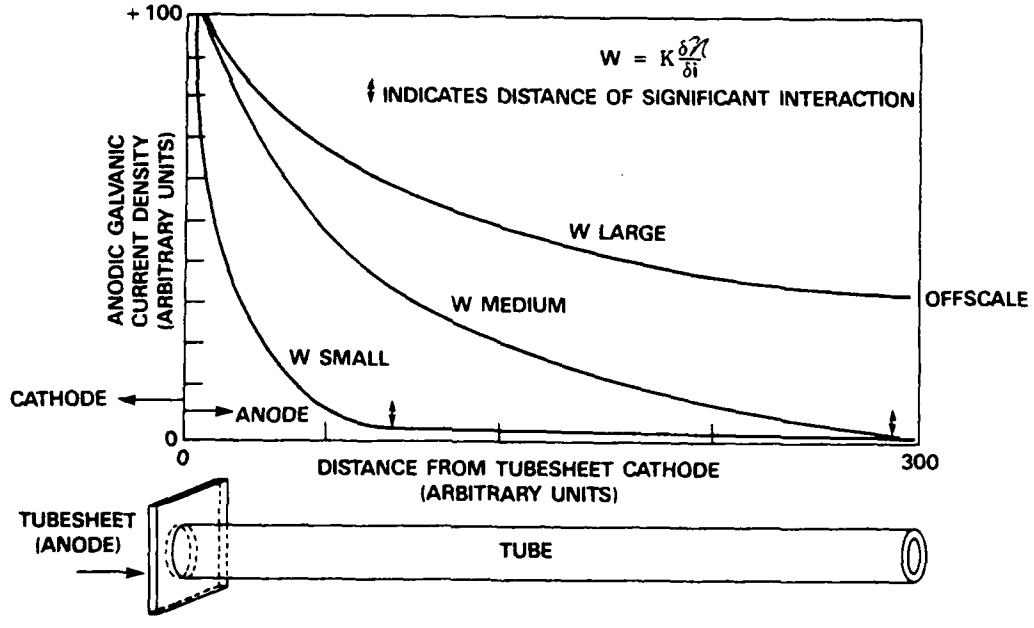

Fig. 19. Schematic galvanic current versus distance plot for an anode tube coupled to a cathode tubesheet for various magnitudes of the Wagner polarization parameter.

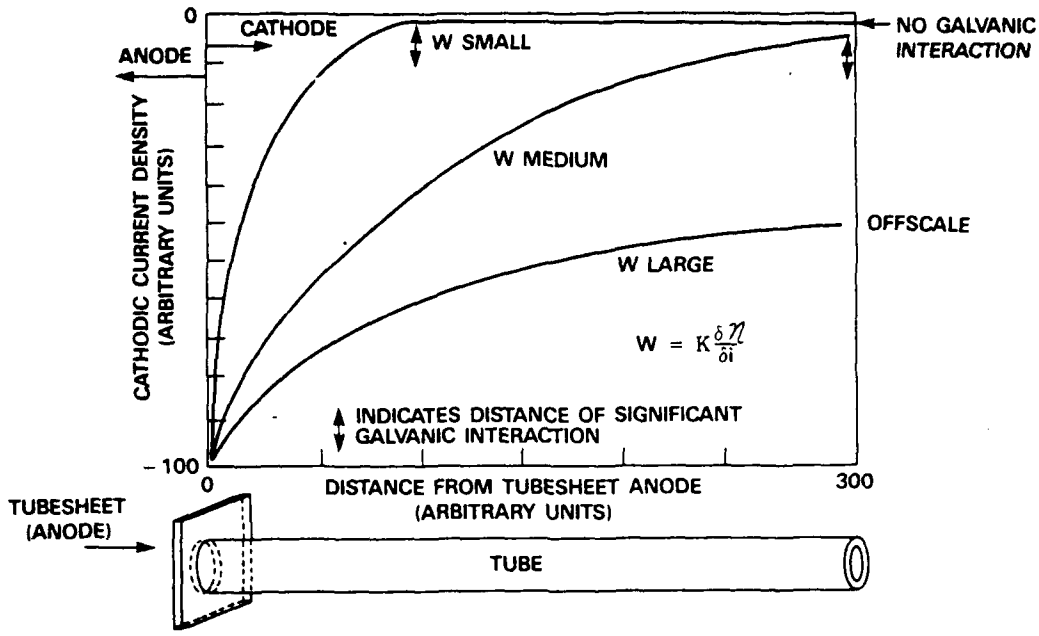

Fig. 20. Schematic galvanic current versus distance plot for a cathode tube coupled to an anode tubesheet for various magnitudes of the Wagner polarization parameter.

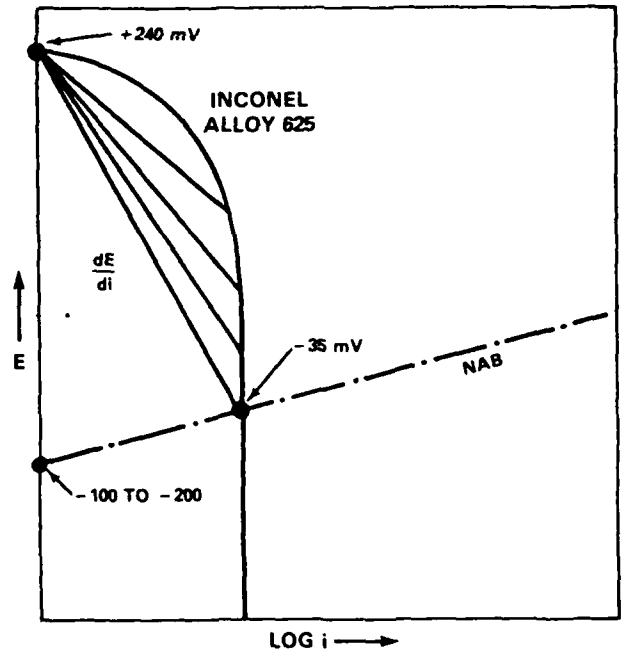

Fig. 21. Schematic E versus log i plot describing galvanic corrosion behavior of alloy 625 coupled to Ni-Al-bronze.

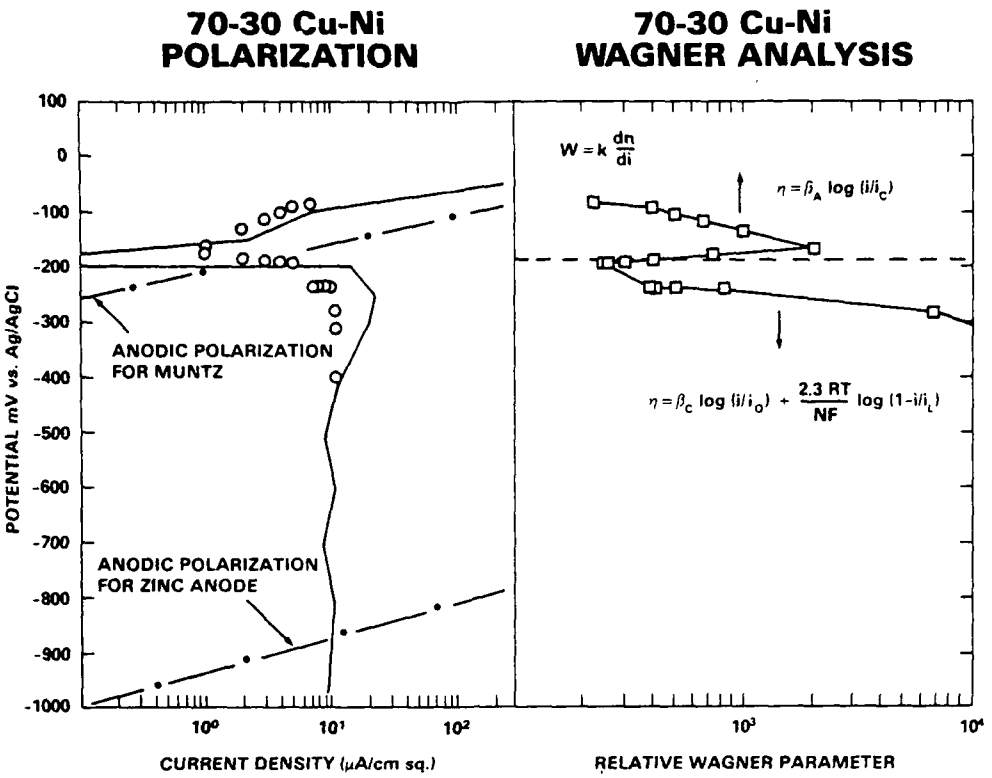

Fig. 22. Polarization plot and Wagner polarization analysis for a Cu-Ni alloy in quiescent seawater.

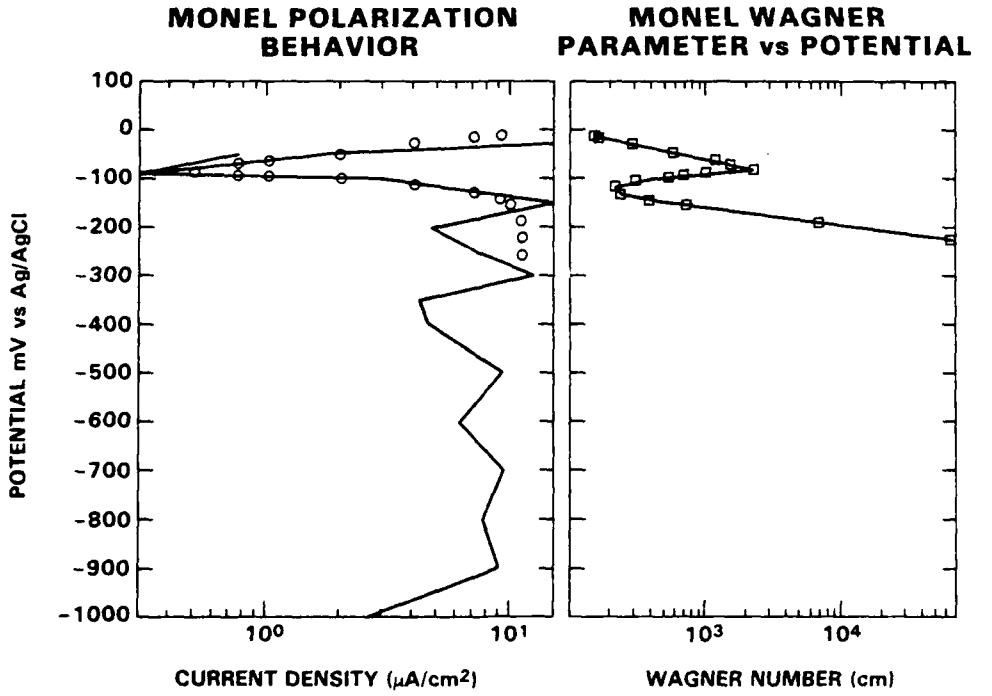

Fig. 23. Polarization plot and Wagner polarization analysis for Monel alloy 400 in quiescent seawater.

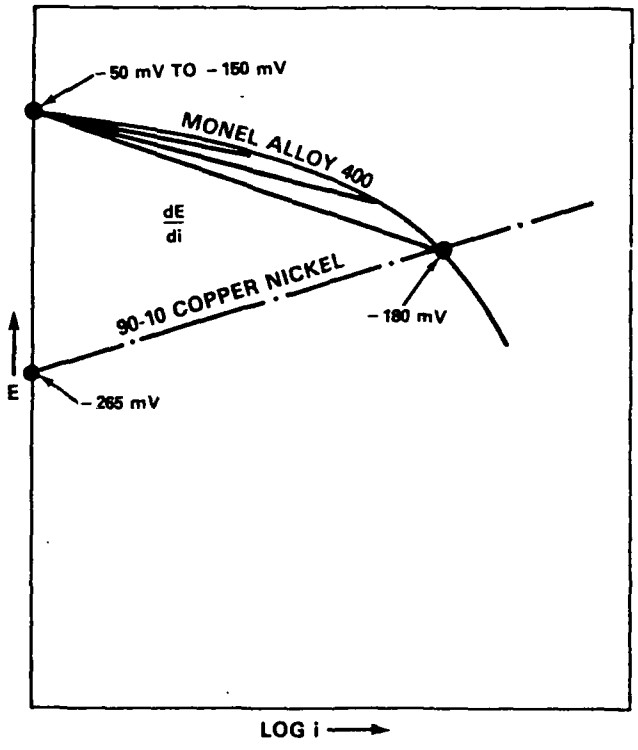

Fig. 24. Schematic E versus log i plot describing galvanic corrosion behavior of Monel alloy 400 coupled to 90-10 Cu-Ni.

REFERENCES

1. Hack, H.P. and J.R. Scully, "Galvanic Corrosion Prediction Using Long-Term Potentiostatic Polarization Curves," Corrosion, Vol. 42, No. 2, p. 79 (1976).
2. Scully, J.R. H.P. Hack, and G.D. Tipton, Corrosion, Vol. 42, No. 8, p. 462 (1986).
3. Gehring, G.A., C.K. Kuester, and J.R. Maurer, Corrosion/80, Chicago, Paper 32 (1980).
4. Gehring G.A. Jr., "Galvanic Corrosion of Selected Tubesheet/Tube Couples under Simulated Seawater Condenser Conditions," Corrosion/81, Toronto, Canada (Apr 1981).
5. Gehring, G.A. and R.J. Kyle, Jr., "Galvanic Corrosion in Steam Surface Condensers Tubed with Either Stainless Steel or Titanium," Corrosion/82, Houston, TX (Mar 1982).
6. Astley, D.J., "A Method for Calculating the Extent of Galvanic Corrosion and Cathodic Protection in Metal Tubes Assuming Undirectional Current Flow," Corrosion Science, Vol. 23, No. 8, pp. 801-832 (1983).
7. Fu, J.W., Technical Note, "A Finite Element Analysis of Corrosion Cells," Corrosion, Vol. 38, No. 5, p. 295 (May 1982).
8. Fu, J.W., "A Finite Element Analysis of Corrosion Cells with Mathematical as Well as Experimental Verifications," Scientific Paper 80-IDZ-MEEIC-P1.
9. Fu, J.W. and J.S.K. Chow, "Cathodic Protection Designs Using on Integral Equation Numerical Method," Materials Performance, p. 9. (Oct 1982).
10. Kasper, R.G. and M.G. April, "Electrogalvanic Finite Element Analysis of Partially Protected Marine Structures," Corrosion, Vol. 39, No. 5, p. 181 (May 1983)
11. Strommen, R. and A. Rodland, "Computerized Techniques Applied in Design of Offshore Cathodic Protection System," Materials Performance, p. 15 (Apr 1981).
12. Munn, R.S., "A Mathematical Model for Galvanic Anode Cathodic Protection System," Materials Performance, p. 29 (Aug 1982).

13. Decarlo, E.A., "Computer Aided Cathodic Protection Design Technique for Complex Offshore Structures," Corrosion/82, Paper 165, Houston, TX (22-26 Mar 1982).

14. Doig, P. and P.E.J. Flewitt, "A Finite Difference Numerical Analysis of Galvanic Corrosion for Semi-Infinite Linear Coplanar Electrodes," J. Electrochem, Soc., p. 2057 (Dec 1979).

15. Wagner, C., J. Electrochem. Soc., Vol. 98, No. 116 (1951).

16. Wagner, C. and W. Traud, Z. Electrochem. Bc-Bunsenges Phys. Chem., p. 44 (1938).

INITIAL DISTRIBUTION

Copies

1 Commander
Naval Ocean Systems Center
San Diego, CA 92152
Attn: Mr. Gordon Chase
Code 932

1 Office of Naval Research
800 N. Quincy St.
Arlington, VA 22217
Attn: Dr. J. Sedriks, Code 1131

1 Office of Naval Technology
800 N. Quincy St.
Arlington, VA 22217
Attn: Mr. J.J. Kelly

1 Commander
Naval Surface Weapons Center
Dahlgren, VA 22448
Attn: Dr. S. Bettadapur
Code G53

2 Commander
Naval Surface Weapons Center
Silver Spring, MD 20910
Attn: Dr. C. Dacres
Code R33
Dr. J. Tydings
Code R32

2 Commander
Naval Air Development Center
Warminister, PA 18974
Attn: Dr. V. Agarwala
Code 6062
Mr. S. Schaffer
Code 6062

2 Commander
Naval Civil Engineering Lab.
Port Hueneme, CA 93043
Attn: Mr. J. Jenkins
Mr. Brunner

Copies

1 Commanding Officer
Air Force Materials Lab.
Wright-Patterson Air Force Base
Dayton, OH 45433
Attn: Mr. F. Meyer
Code MLSA

2 Department of the Army
AMTL
SLCMT-MCM-SB
Watertown, MA 02172
Attn: Mr. M. Levy
Ms. N, Kackley

1 National Bureau of Standards
Washington, DC 20234
Attn: Dr. N.E. Pugh

1 Commander
Naval Underwater Systems Center
New London, CT
Attn: Dr. R. Kasper

2 ONR

7 NAVSEA
1 SEA 05
2 SEA 05R25
2 SEA 05M1
2 SEA 99612
1 SEA 56N3

2 DTIC

DISTRIBUTION (Continued)

CENTER DISTRIBUTION

Copies	Code
1	012 (Caplan)
1	1508
1	28
1	2801
3	2803
1	2809
5	281
5	2813 (Morton)
10	2813 (Hack)
1	284
1	2841
1	522.2 (TIC)
2	5231

END

DATE

FILMED

9-88

DTIC